Resonance effects in the $5\sigma^{-1}$ photoionization channel of CO

M. R. F. Siggel, M. A. Hayes, M. A. MacDonald, and J. B. West
Daresbury Laboratory, Daresbury, Warrington WA4 4AD, United Kingdom

J. L. Dehmer
Argonne National Laboratory, Argonne, Illinois 60439

A. C. Parr and J. E. Hardis
National Institute for Standards and Technology, Gaithersburg, Maryland 20899

I. Iga
Departamento de Quimica, Universidade Federal de São Carlos, Via Washington Luiz 13560, Brazil

V. Tiit
Institute of Physics, 202400 Tartu, Estonia

Vibrational branching ratios and photoelectron angular distributions are reported for the $5\sigma^{-1}$ photoionization channel of CO in the range 16 eV $< h\nu <$ 45 eV. Striking non-Franck–Condon effects are observed in both the branching ratios and angular distributions as a result of various autoionizing states and a σ shape resonance that lie in this spectral range. The goal of the present measurement was to observe definitive evidence for the σ shape resonance via its non-Franck–Condon effects on the vibrational ionization channels. Guided by recent calculations [Smith, Lynch, and McKoy, J. Chem. Phys. **85**, 6455 (1986)], we examined the broad structure in the vibrational branching ratios and angular distributions in the range 25 eV $< h\nu <$ 40 eV. There, we found clear evidence for the σ shape resonance in the quantities $\beta(v^+ = 0$ and 1$)$ and $\sigma(v^+ = 2)/\sigma(v^+ = 0)$. Substantial differences between theory and experiment for the $\sigma(v^+ = 1)/\sigma(v^+ = 0)$ branching ratio, however, serve to define the limitations of the current single-channel picture for this process.

I. INTRODUCTION

Shape resonances are localized, quasibound states whose distinctive properties have proven very useful in the study of the interaction of excited electrons with anisotropic molecular fields (see, e.g., Refs. 1 and 2). Of particular interest here is the acute sensitivity of a shape resonance to variations of internuclear separation along any bond with which it has significant spatial overlap. This sensitivity was predicted[3] many years ago to induce non-Franck–Condon (non-FC) effects in molecular photoionization. In particular, photoionization channels containing shape resonances are expected to exhibit non-FC vibrational branching ratios and v-dependent photoelectron angular distributions over a spectral range much broader than the resonance halfwidth.

This effect arises from the quasibound nature of the shape resonance, which is localized in a spatial region of molecular dimensions by a centrifugal barrier. This barrier and, hence, the energy and lifetime (width) of the resonance are sensitive functions of internuclear separation (R) and vary significantly over a range of R corresponding to the ground state vibrational motion. In an adiabatic treatment,[3-5] the net dipole amplitude for a particular vibrational channel is obtained by averaging the R-dependent dipole amplitude, weighted by the product of the initial- and final-state vibrational wave functions at each R. Accordingly, transitions to alternative vibrational levels of the ion preferentially weight different regions of R, leading to resonance positions and widths that vary with vibrational channel.

When cast as ratios of vibrational intensities, this leads to large systematic deviations from the constant FC ratio that would apply if the electronic and nuclear motions were independent. It also leads to v-dependent photoelectron angular distributions, rather than the v independence that would obtain in the FC approximation.

The initial theoretical predictions[3-5] concerned the σ_u shape resonance in $3\sigma_g^{-1}$ photoionization of N_2. Subsequent measurements of the vibrational branching ratios[6] and photoelectron angular distributions[7] confirmed the shape-resonance-induced effects. The first attempt to verify the shape resonance effect in vibrational branching ratios was, however, performed[8] on the analogous σ shape resonance in the $5\sigma^{-1}$ channel of CO, which lay in a more convenient wavelength range for normal incidence monochromators. Indeed, non-FC effects were observed that qualitatively resembled those predicted for N_2. However, subsequent calculations[9,10] failed to reproduce the observations, indicating instead that the shape resonance effect was spread out over a much broader energy range than were the observed variations. A similar statement describes the corresponding studies of the photoelectron angular distributions.[9-11] In retrospect, it is now clear that the experimental observations were significantly affected by the presence of a doubly excited valence state at ~21–22 eV, which has been suggested[9] to be analogous to the prominent doubly excited state in N_2 at 23 eV.[12] In addition, it is now well established (see, e.g., Refs. 13–33) that there are several multiply excited states of CO^+ in the energy range 22 eV $< h\nu <$ 40 eV, so that observ-

able effects of the autoionizing states converging to these limits are also possible. Some of these states have been observed as very weak structure in the absorption spectrum.[14,17,32] Consequently, whereas the present study seeks to identify the underlying shape resonance behavior in the observed non-FC effects, it bears keeping in mind that the continuum states in this spectral range are eigenstates of a multichannel system containing closed as well as open continuum channels.

Despite these complexities, the shape resonance effects may be characterized on the following basis. The non-FC effects resulting from autoionization will be concentrated in the spectral region near the relatively narrow autoionizing states, whereas the shape-resonance-induced non-FC effects can extend over a spectral range many times the full width at half-maximum (FWHM) of the resonance itself, which in this case is over 5 eV. Hence, the shape resonance effect may extend well beyond localized effects of autoionization, permitting the identification and study of the gross spectral behavior of the well-known σ shape resonance in CO through its influence on the vibrational channels. (Note that in the case of N_2, the two types of resonances are more separated in the spectrum, so that their individual study was more straightforward.[3-7]) Indeed, recent calculations[10] give guidance as to the best strategy for observing the shape resonance effects. The asymmetry parameter for the $v^+ = 0$ and 1 channels exhibit broad minima near 30 eV. Of these two, the $v^+ = 1$ is the more distinct, providing the best opportunity for observing the shape resonance. Note that the β for $v^+ = 2$ has a minimum in the midst of the autoionization structure and is therefore of little use for the present purposes. The branching ratios are somewhat less promising, but they also exhibit characteristic behavior. The $v^+ = 1/v^+ = 0$ ratio peaks at approximately 25 eV, which is rather close to the previously observed peak at 22 eV, caused by autoionization. The $v^+ = 2/v^+ = 0$ ratio peaks at approximately 29 eV, making it of possible use, although its 1% magnitude makes its spectral shape somewhat difficult to characterize. Indeed, we do find the signature of the σ shape resonance in three of the four observables examined, while the $v^+ = 1/v^+ = 0$ ratio departs qualitatively from predictions. These results stress the importance of both vibrationally resolved photoelectron spectroscopy and a broad spectral perspective for resolving resonance effects in molecular photoionization.

II. EXPERIMENT

The electron spectrometer used in this investigation was constructed jointly by the National Institute of Standards and Technology and Argonne National Laboratory. It comprises two hemispherical electron analyzers, both arranged to detect electrons ejected at right angles to the incoming photon beam. One analyzer was fixed in position, accepting electrons ejected horizontally, and the other was rotatable about the light beam through an angular range of a little more than 90° from a vertical orientation. The angular acceptance of the analyzers was limited by apertures to approximately ± 2°. Photoelectrons were detected by area de-

tectors with resistive anode encoders. The sample gases were of research grade and were introduced into the experimental chamber through a 0.25 mm capillary, providing an effusive source. A capillary light guide of 2 mm diameter channeled the vacuum ultraviolet (vuv) radiation from the exit slit of the optical monochromator to a point near the gas source, forming an interaction region "viewed" by both analyzers. The vuv radiation was provided by the Synchrotron Radiation Source at Daresbury Laboratory, a 2 GeV electron storage ring. Two sets of measurements are presented, using two different monochromators: a 5 m normal-incidence monochromator (NIM) and a toroidal grating monochromator (TGM). The two data sets are identified in the figures by different symbols, with the NIM data covering the range 10–25 eV and overlapping with the TGM data, which extend to 40 eV. Further details of the electron spectrometer system have been published by Parr et al.[34] The only difference between the system in its present form and the one described earlier is the use of area detectors instead of channeltrons at the exit planes of the hemispheres. A description of the NIM and its performance was given by Holland et al.,[35] and of the TGM and the beam line to which all of this equipment was fitted, by West and Padmore.[36]

The radiation leaving the exit slit of the monochromator is elliptically polarized, the major axis of the ellipse being horizontal. The polarization measurement was made in two different ways for the two monochromators. In the case of the NIM, the polarization analyzer built into the system was used. This incorporates three mirrors reflecting at angles of 67.5°, 45°, and 67.5° and closely follows the principle described by Horton et al.[37] A tungsten mesh served as a flux monitor for the radiation entering this detector, and a tungsten plate was used to measure the intensity after the three reflections. By making measurements at 0° and 90°, and from a knowledge of the gold reflectivities for parallel and perpendicular incident light, it is a straightforward matter to calculate the polarization. This analyzer was less reliable for the TGM, because the photon flux from this instrument is generally lower than that from the NIM, and the analyzer itself is less efficient at the higher photon energies. For the TGM helium was used to determine the polarization for photon energies above 25 eV, by measuring the electron count rate from the rotatable analyzer at its 0° and 90° positions and taking advantage of the fact that the photoelectron asymmetry parameter, β, has a value of 2 for helium. Argon was used below 25 eV in the same fashion, using the argon β parameters published by Holland et al.[38] Any slight change in efficiency of the rotatable analyzer between the two positions was corrected by measuring the polarization on the NIM with both the reflection analyzer and helium. Under the assumption that the reflection analyzer was correct, this immediately gave the correction required. In practice, the difference in efficiency between the two positions was <5%.

The relative efficiency of the analyzers as a function of electron kinetic energy must also be measured, and this was done by measuring the intensities from ionization of the outer electrons in the rare gases as a function of photoelectron energy and comparing those with the known photoionization cross sections at the corresponding photon energies. In

doing this, the electron signal is referenced against the incident flux monitor, the tungsten mesh in the polarization analyzer. The variation of the efficiency of this detector with photon energy was measured in a separate experiment. The expression

$$\frac{d\sigma}{d\Omega} = \frac{\sigma}{4\pi} \left[1 + \frac{\beta}{4} \left(3p \cos 2\theta + 1 \right) \right] \qquad (1)$$

for the differential cross section was needed to account for the effects of angular distribution, contained in the β parameter, and of polarization p of the incoming light. In this expression,[39-41] θ is the angle between the major polarization component and the outgoing electron direction, and σ is the partial cross section for that channel. Where helium is used as the calibrant gas, β can be assumed to take the value 2. Thus the relative energy calibration does not depend on measured values of the β parameter. For the measurements presented here, both argon and helium were used.

The use of area detectors, in place of the more usual single-channel electron multiplier, introduces a further calibration issue because the efficiency of the detector varies over its surface. To account for this variation, it is also necessary to know the electron energy dispersion of the hemispherical analyzers at their exit planes. This dispersion was measured by using argon gas, by observing the correlation between the positions of the $^2P_{1/2,3/2}$ photoelectron peaks and the retarding potential applied to the electrons entering the lens system. This information, in the form of a dispersion table, was then used in the main software routine for data taking, in which electron spectra were scanned and summed across the plates so that each part of the spectrum saw all the active area of the detector. This procedure corrected for any variations in efficiency across the detector.

The resolution of the optical monochromator used throughout these experiments was about 10 meV for the NIM and 50 meV for the TGM, sufficient therefore to resolve the vibrational structure in CO when combined with an electron spectrometer resolution of 40 meV. The raw data were corrected for the energy response and relative efficiencies of the electron analyzers, and the intensities in the vibrational peaks were found by using a Gaussian least squares fitting procedure. The value of β for each vibrational member was derived from the ratio of the intensities from each analyzer, using Eq. (1). Once β was known, the intensity integrated over all θ in a given vibrational member could be found. This intensity is proportional to the partial cross section, and we used it to calculate branching ratios, defined in this work as the intensity observed in a particular vibrational member divided by the intensity of the first vibrational member.

III. RESULTS AND DISCUSSION

The present results are shown in Figs. 1–4, together with the earlier synchrotron data and the results of calculations of the shape-resonance-induced non-FC effects in the independent electron approximation. The $v^+ = 1/v^+ = 0$ and $v^+ = 2/v^+ = 0$ vibrational branching ratios are presented in Figs. 1 and 2; and the photoelectron asymmetry param-
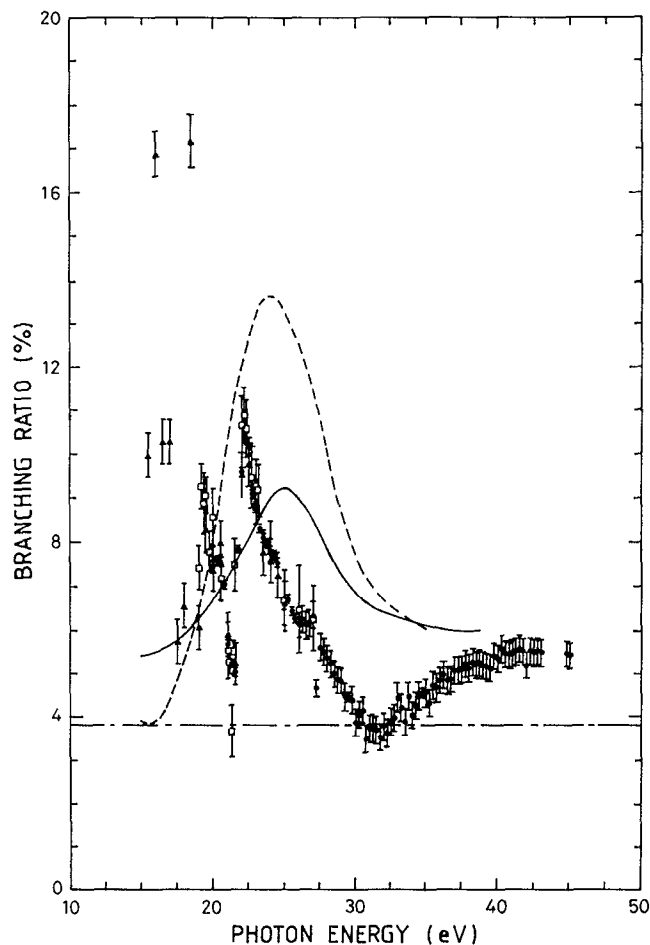

FIG. 1. The CO^+ $X^2\Sigma^+$ $v^+ = 1/v^+ = 0$ branching ratio for $5\sigma^{-1}$ photoionization of CO: ▲, present NIM data; ●, present TGM data; □, data from Ref. 8; ---, multiple scattering model calculation, Ref. 9; —, variational Schwinger calculation (dipole length), Ref. 10; – – –, Franck–Condon factor.

eters (β) for $v^+ = 0$ and 1 are presented in Figs. 3 and 4, respectively. In each figure the same conventions are used to designate the three data sets and two theoretical curves. The present data are represented by solid circles for the TGM experiment and by solid triangles for the NIM experiment. Open squares denote the earlier synchrotron radiation results[8,11] in the range $h\nu = 19$ to 27 eV. The two theoretical curves are shown as dashed and solid lines for the multiple-scattering[9] and dipole-length variational Schwinger[10] calculations, respectively. There are some earlier vibrational branching ratio,[42,43] partial cross section,[44,45] and angular distribution measurements[43,46] using resonance radiation and synchrotron radiation, but they do not help to establish the broad shape of these quantities over the energy range of interest here and would be difficult to discern amidst the present data. Finally, Fig. 1 shows the constant 3.8% ratio of Franck–Condon factors in order to underscore the departure of the present results from the behavior expected in the Franck–Condon approximation. The ~0.02% FC ratio for $v^+ = 2/v^+ = 0$ is too small to be seen clearly in Fig. 2.

Before discussing these results, we will briefly review the ion states and different ionization mechanisms that may pos-
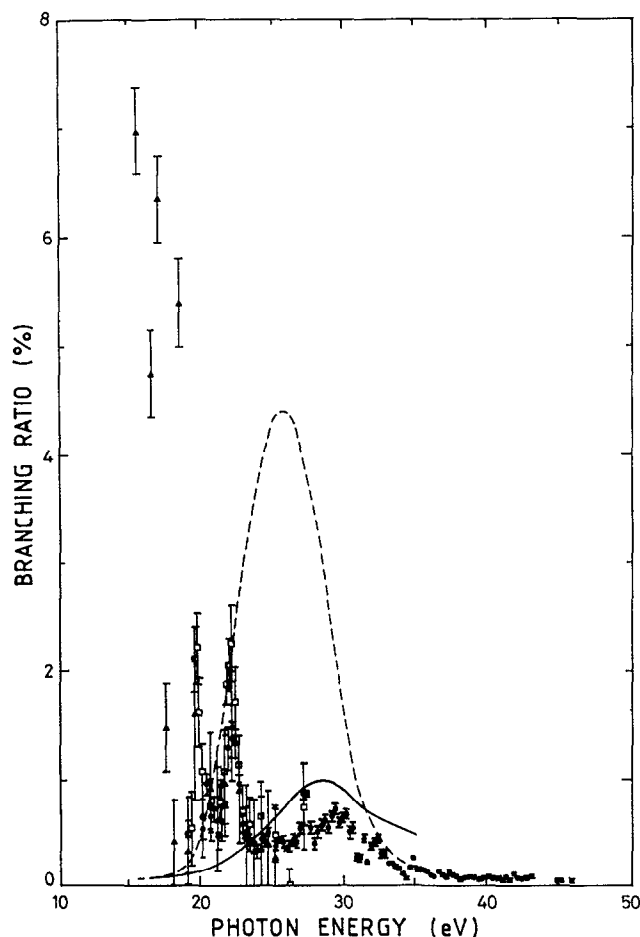
FIG. 2. The CO^+ $X^2\Sigma^+$ $v^+ = 2/v^+ = 0$ branching ratio for $5\sigma^{-1}$ photoionization of CO: ▲, present NIM data; ●, present TGM data; □, data from Ref. 8; ---, multiple scattering model calculation, Ref. 9; —, variational Schwinger calculation (dipole length), Ref. 10.
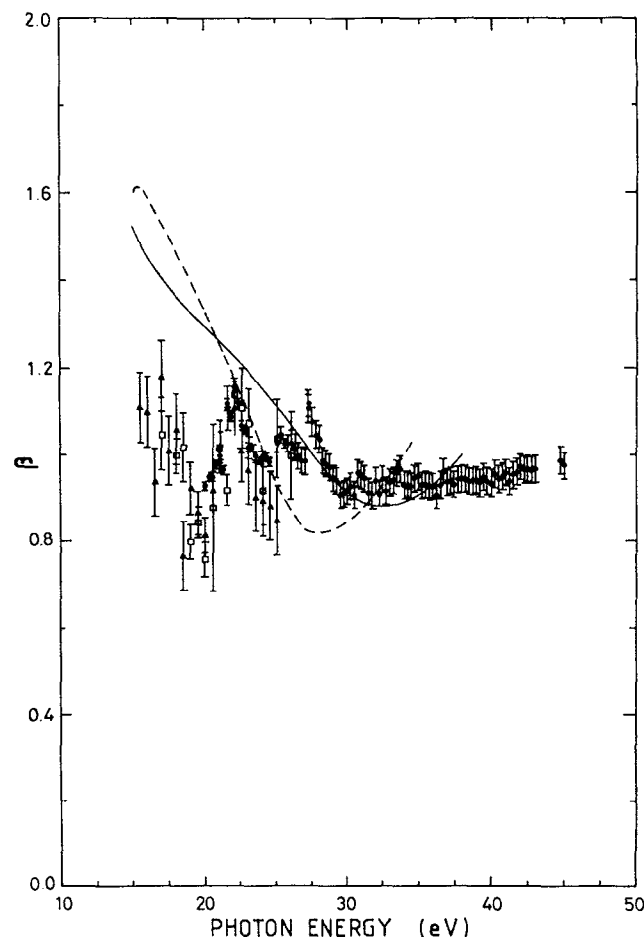

FIG. 3. Photoelectron asymmetry parameter, β, for CO^+ $X^2\Sigma^+$ $v^+ = 0$ from $5\sigma^{-1}$ photoionization of CO: ▲, present NIM data; ●, present TGM data; □, data from Ref. 11; ---, multiple scattering model calculation, Ref. 9; —, variational Schwinger calculation (dipole length), Ref. 10.

sibly contribute to the vibrational ionization channels observed in these measurements. The electronic configuration of the ground state of CO is[15] $KK(3\sigma)^2(4\sigma)^2(1\pi)^4(5\sigma)^2$. Removal of an electron from the 5σ, 1π, 4σ, and 3σ orbitals produces the following electronic states of CO^+ (vertical ionization potentials,[15] IPs, in parentheses): $X^2\Sigma^+$ (14.5 eV), $A^2\Pi$ (17.2 eV), $B^2\Sigma^+$ (20.1 eV), and $(3\sigma)^{-1}\,^2\Sigma^+$. Since the photoelectron spectra recorded in this experiment select vibrational components of the ground state of CO^+, the direct photoionization channels of interest are $5\sigma \to \epsilon\sigma$, $\epsilon\pi$. It is the $\epsilon\sigma$ continuum that exhibits a prominent shape resonance[9,10,47] at a kinetic energy of ~ 12 eV above the 5σ IP. It is the $l = 3$ component of the $\epsilon\sigma$ wave function that resonates, although mixing with the $l = 0,1$, and 2 components does occur.[45] Actually, the exact energy of the shape resonance is not accurately known in the $5\sigma^{-1}$ channel, because it is not easy to separate from autoionization structure in the absorption or partial cross section data. Therefore, in addition to measuring the characteristic fingerprint of the shape resonance, we are seeking a clear observation of its location.

In addition to direct ionization, there are indirect mechanisms for producing the observed ionization channels. This can arise, for example, from the excitation and decay of auto-ionization states converging to ionic states in this energy range. Besides the single-hole ion states listed above, there are a number of additional states[13-33] between 20 and 40 eV. These result[23,24,26,31] from strong correlation effects that mix single-hole states, two-hole one-particle states, and certain higher-order hole–particle combinations. These many-body effects cause a breakdown of the single-particle model and appear to be a common aspect of inner-valence spectra of molecules. These multiply excited states have been discussed extensively in the literature;[13-33] however, the assignments are not yet completely consistent. We summarize the assignments (vertical IPs in parentheses) using the convention of Wu,[32] which is drawn from the recent theoretical analysis of Langhoff et al.:[31] $C^2\Sigma^+$ (22.73 eV), $D^2\Sigma^+$ (23.38 eV), $E^2\Pi$ (25.48 eV), $F^2\Pi$ (28.1 eV), $G^2\Sigma^+$ (31.8 eV), and $H^2\Sigma^+$ (37.3 eV). Converging to each of these will be neutral Rydberg states that may decay by autoionization, if they are symmetry allowed, into the $X^2\Sigma^+$, $v^+ = 0,1$ continua. In any event, they will cause effects that are localized to the vicinity of the relatively narrow (compared to the scope of this study) autoionizing states. A small number of these states have appeared as very weak features in the absorption
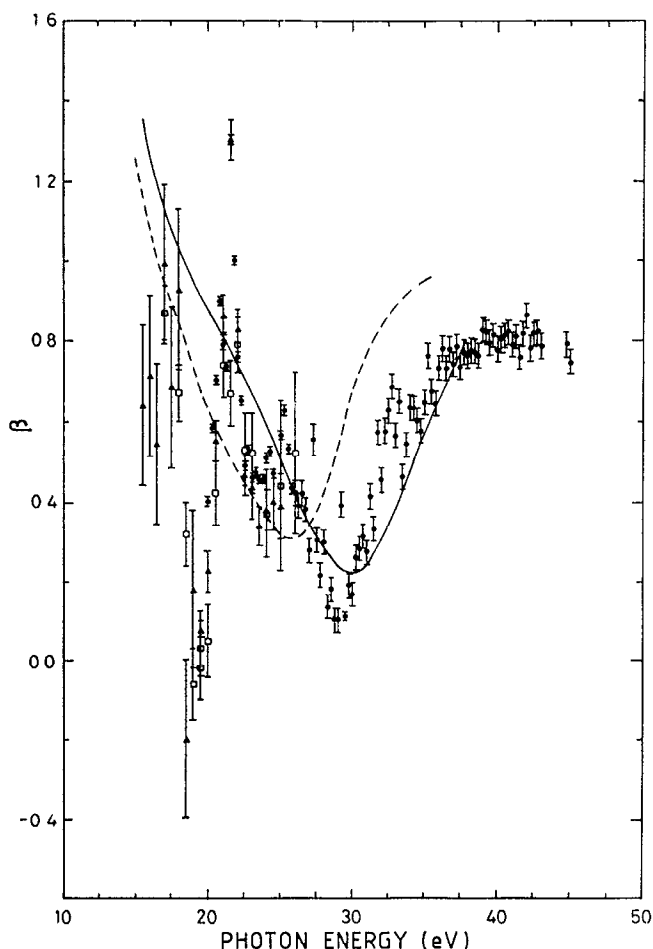
FIG. 4. Photoelectron asymmetry parameter, β, for CO^+ $X\,^2\Sigma^+$ $v^+ = 1$ from $5\sigma^{-1}$ photoionization of CO: ▲, present NIM data; ●, present TGM data; □, data from Ref. 11; ---, multiple scattering model calculation, Ref. 9; —, variational Schwinger calculation (dipole length), Ref. 10.

cross section.[14,17,32] The prominent valence state observed in all observables at ~ 21–22 eV can be thought of as a doubly excited precursor to one or more of these Rydberg series. The latter is likely to be much weaker, however, because one of the electrons will be promoted from a localized valence orbital to a diffuse Rydberg orbital. Finally, it has also been well documented[21,22,30,32,33] that several dissociative ionization and double ionization channels open up in the range studied.

These potential complexities notwithstanding, the point of the present study is to examine the non-FC effects in this channel over a broad, 30 eV, energy range so that the broad, characteristic shape resonance behavior might emerge from the other more localized and presumably weak mechanisms that are known to occur above the prominent valence state at ~ 21–22 eV. This goal is best achieved in the $\beta(v^+ = 1)$ data shown in Fig. 4. The spectral dependence of this quantity clearly shows two prominent resonant structures, the large oscillation centered at ~ 21 eV and the broad dip centered at 29 eV. It is the broad feature at higher energy that we

ascribe to the $\epsilon\sigma$ shape resonance, rather than the autoionization structure mistakenly identified as such in the earlier study.[8,11] There are some localized fluctuations in the gross variation of the experimental curves, tempting one to consider some of the mechanisms discussed in the last paragraph; however, the data quality does not justify any conclusions of this type. The three data sets in Fig. 4 are in good agreement. The two theoretical curves in Fig. 4 agree qualitatively with each other and with the broad minimum in the data. The variational Schwinger calculation[10] is in much better agreement with experiment than is the earlier multiple-scattering calculation.[9] In fact, the location of the minimum in Fig. 4 gives an indication of the position of the shape resonance in this channel: The minimum in the experimental curve lies at ~ 29 eV, while the dipole-length calculation of Smith *et al.*[10] lies at 30 eV. On this basis, we conclude that the shape resonance lies ~ 1 eV below its position in that calculation, or at ~ 25 eV in the vibrationally unresolved photoionization cross section, a conclusion that could not be drawn from the photoionization cross section because of interference from autoionizing structure in the vicinity of the maximum. This estimate must be considered approximate, however, both because the continuum wave functions in the vicinity of the shape resonance maximum will be influenced by indirect as well as direct photoionization processes, and because alternative observables reflect the dynamics differently, so that agreement between experiment and theory in one variable does not assure agreement in another.

The $v^+ = 2/v^+ = 0$ vibrational branching ratio in Fig. 2 also clearly displays the underlying shape resonant behavior in the broad enhancement at ~ 29 eV, in addition to the autoionization structure at ~ 22 eV. Again, there is good agreement between the earlier data and the two independent measurements reported here. The theoretical curves are in gross qualitative agreement with experiment; however, only the variational Schwinger calculation[10] gives a realistic magnitude for the enhancement of the $v^+ = 2$ channel relative to the $v^+ = 0$ channel. For this branching ratio, the maximum in the calculation by Smith *et al.*[10] appears to occur slightly below the poorly defined maximum in the experimental data. Note that most of the magnitude of the $v^+ = 2$ branching ratio throughout the spectral range in Fig. 2 is induced by one resonant mechanism or another, since the FC value for this ratio is $\sim 0.02\%$, which is approximately the value attained by the experimental data at energies above $h\nu \sim 37$ eV.

The results for $\beta(v^+ = 0)$ are presented in Fig. 3, where three things are immediately obvious: First, the photoelectron asymmetry in the $v^+ = 0$ channel is much greater that that in the $v^+ = 1$ channel. This is significant because the dependence of β on v^+ over a broad energy range is strong evidence for shape-resonance-induced non-FC effects.[3] Second, fairly good agreement is observed among the two data sets reported here and in the earlier measurements of Cole *et al.*[11] and Marr *et al.*[46] The relatively large error bars on the higher energy NIM data is ascribed to uncertainty in the light polarization determination for this run. Third, the TGM data agrees qualitatively with both calculations at higher energies; but, again, only the variational Schwinger

calculation[10] is in semiquantitative agreement with the data. In fact, the agreement in magnitude is very good, although the experimental data exhibits a much weaker rise at high energies than do the calculations. This makes it difficult to discuss the energy position of the characteristic minimum for this observable.

Finally we discuss the $v^+ = 1/v^+ = 0$ branching ratio in Fig. 1. There, the three data sets are seen to be in very good agreement. The branching ratio exceeds the 3.8% ratio of the FCFs over the entire range studied, suggesting resonant enhancement of the $v^+ = 1$ channel by shape and autoionizing resonances. However, in this case the experimental and theoretical curves qualitatively disagree with one another. The calculations exhibit the same shape, but different magnitudes. Both predict an enhancement near the peak of the shape resonance, with a fairly symmetric falloff toward the FC ratio at higher and lower energies. The experimental data, in contrast, contains rather sharp variations in the vicinity of the valence state and other unresolved autoionizing states below ~ 22 eV and then exhibits a broad minimum at $hv \sim 32$ eV, where the calculations are smoothly declining. The data recovers from the minimum to approximately converge with the theoretical curves above 40 eV. Nevertheless, this branching ratio stands out as a major exception to the ability of the independent-electron calculations to account for the broad structure above 22 eV in the vibrational branching ratios and photoelectron angular distributions. At this time, we do not have any explanation for this difference. We note that this branching ratio is a ratio of the partial cross sections for the $v^+ = 1$ and $v^+ = 0$ ionization channels, and therefore the disagreement could arise from a difference in shape of either or to a shift of the two curves. Since the $v^+ = 2/v^+ = 0$ ratio showed reasonable agreement between experiment and theory, one is led to assume that the computed shape of the $v^+ = 0$ partial cross section above 22 eV is reasonably accurate. Another possibility is influence by the valence state at ~ 22 eV. Since the peak in the branching ratio is very near the valence state, significant interaction is to be expected. The peak in the $v^+ = 2/v^+ = 0$ branching ratio occurred at $hv = 29$ eV, which is better separated from the influence of this state. Nevertheless, theory and experiment still depart markedly even above 30 eV, indicating that the independent model has failed to account for all of the essential dynamics governing this observable. In a recent study of non-FC effects in the $4\sigma^{-1}$ photoionization channel of CO, Kakar *et al.*[48] observed a feature that they attributed to the $\epsilon\sigma$ shape resonance in the $5\sigma^{-1}$ channel, which influenced the $4\sigma^{-1}$ channel by continuum–continuum coupling.[49,50] In the spirit of pure speculation, we point out that the $\epsilon\sigma$ shape resonance in the $4\sigma^{-1}$ channel is a broad feature centered[48] at ~ 37 eV and, if it were to couple efficiently to the $v^+ = 1$ ionization channel studied here, it would alter the independent-electron behavior somewhere in the range 30–50 eV. Taken together, the good agreement between experiment and theory discussed above for three parameters and the disagreement for a fourth stresses both the importance of examining complementary observables and the importance of examining molecular photoionization dynamics on the vibrationally resolved level.

IV. CONCLUSIONS

We have presented the vibrational branching ratios and vibrationally resolved photoelectron angular distributions for $5\sigma^{-1}$ photoionization of CO over the spectral range 16 eV $< hv <$ 45 eV. The main purpose was to reexamine and extend an earlier study[8,11] of striking non-FC effects in this channel in order to gain the perspective necessary to identify the signature of the $\epsilon\sigma$ shape resonance in the presence of the autoionization and other processes occurring in this energy region. This goal was in large part attained as three out of four of the observables examined clearly displayed prominent, relatively narrow structure near 22 eV, believed to represent an autoionizing valence state, and broad structure from 23 to 45 eV, which exhibited the characteristic shape-resonant behavior predicted by independent-electron calculations. In particular, the variational Schwinger calculation by Smith *et al.*[10] agrees very closely with experiment above 23 eV. The shifts between experiment and theory were smaller than ~ 1 eV, indicating that this calculation represents the shape resonance in this channel with an unusually high degree of accuracy. In sharp departure from this sense of growing understanding, the measured $v^+ = 1/v^+ = 0$ branching ratio departed strongly from the theoretical predictions. Even in the energy range above 30 eV, the experiment and theory produced qualitatively different trends, which only seemed to converge at the high energy limit of the present study. We believe that this rather intriguing puzzle underscores the complementary nature of these closely related observables, and we hope that these data stimulate further theoretical studies of the interplay between shape resonances, autoionizing resonances, and other mechanisms in this oft-studied photoionization channel in CO.

ACKNOWLEDGMENTS

[1] J. L. Dehmer, A. C. Parr, and S. H. Southworth, in *Handbook on Synchrotron Radiation*, Vol. II, edited by G. V. Marr (North-Holland, Amsterdam, 1987), p. 241.

[2] V. McKoy, T. A. Carlson, and R. R. Lucchese, J. Phys. Chem. **88**, 3188 (1984).

[3] J. L. Dehmer, D. Dill, and S. Wallace, Phys. Rev. Lett. **43**, 1005 (1979).

[4] G. Raseev, H. LeRouzo, and H. Lefebvre-Brion, J. Chem. Phys. **72**, 5701 (1980).

[5] R. R. Lucchese and V. McKoy, J. Phys. B **14**, L629 (1981).

[6] J. B. West, A. C. Parr, B. E. Cole, D. L. Ederer, R. Stockbauer, and J. L. Dehmer, J. Phys. B **13**, L105 (1980).

[7] T. A. Carlson, M. O. Krause, D. Mehaffy, J. W. Taylor, F. A. Grimm, and J. D. Allen, J. Chem. Phys. **73**, 6056 (1980).

[8] R. Stockbauer, B. E. Cole, D. L. Ederer, J. B. West, A. C. Parr, and J. L. Dehmer, Phys. Rev. Lett. **43**, 757 (1979).

[9] J. A. Stephens, D. Dill, and J. L. Dehmer, J. Phys. B **14**, 3911 (1981).

[10] M. E. Smith, D. L. Lynch, and V. McKoy, J. Chem. Phys. **85**, 6455 (1986).

[11] B. E. Cole, D. L. Ederer, R. Stockbauer, K. Codling, A. C. Parr, J. B. West, E. D. Poliakoff, and J. L. Dehmer, J. Chem. Phys. **72**, 6308 (1980).

[12] G. Wendin, Int. J. Quantum Chem. Quantum Chem. Symp. **13**, 659 (1979).

[13] K. Siegbahn, C. Nordling, G. Johansson, J. Hedman, P. F. Heden, K. Hamrin, U. Gelius, T. Bergmark, L. O. Werme, R. Manne, and Y. Baer, *ESDA Applied to Free Molecules* (North-Holland, Amsterdam, 1969).

[14] M. Sasanuma, E. Ishigura, Y. Morioka, and M. Nakamura, Third International Conference on Vacuum Ultraviolet Radiation Physics, edited by Y. Nakai (Physical Society of Japan, Tokyo, 1971), p. 1pA2–3.

[15] U. Gelius, E. Basilier, S. Svensson, T. Bergmark, and K. Siegbahn, J. Electron Spectrosc. **2**, 405 (1974).

[16] M. Okuda and N. Jonathan, J. Electron Spectrosc. **3**, 19 (1974).

[17] K. Codling and A. W. Potts, J. Phys. B **7**, 163 (1974).

[18] L. Asbrink, C. Fridh, E. Lindholm, and K. Codling, Phys. Scr. **10**, 183 (1974).

[19] A. W. Potts and T. A. Williams, J. Electron Spectrosc. **3**, 3 (1974).

[20] L. C. Lee, R. W. Carlson, and D. L. Judge, Mol. Phys. **30**, 1941 (1975).

[21] A. Hamnett, W. Stoll, and C. E. Brion, J. Electron Spectrosc. **8**, 367 (1976).

[22] G. R. Wight, M. J. van der Wiel, and C. E. Brion, J. Phys. B **9**, 675 (1976).

[23] P. S. Bagus and E.-K. Viinikka, Phys. Rev. A **15**, 1486 (1977).

[24] J. Schirmer, L. S. Cederbaum, W. Domcke, and W. von Niessen, Chem. Phys. **26**, 149 (1977).

[25] E. W. Plummer, T. Gustafsson, W. Gudat, and D. E. Eastman, Phys. Rev. A **15**, 2339 (1977).

[26] L. S. Cederbaum and W. Domcke, Adv. Chem. Phys. **36**, 205 (1977).

[27] J. S. Lee, J. Chem. Phys. **67**, 3998 (1977).

[28] S. Krummacher, V. Schmidt, and F. Wuilleumier, J. Phys. B **13**, 3993 (1980).

[29] B. P. Tsai and J. H. D. Eland, Int. J. Mass Spectrom. Ion Phys. **36**, 143 (1980).

[30] T. Masuoka and J. A. R. Samson, J. Chem. Phys. **74**, 1093 (1981).

[31] P. W. Langhoff, S. R. Langhoff, T. N. Rescigno, J. Schirmer, L. S. Cederbaum, W. Domcke, and W. von Niessen, Chem. Phys. **58**, 71 (1981).

[32] C. Y. R. Wu, J. Chem. Phys. **77**, 1179 (1982).

[33] T. Masuoka, J. Chem. Phys. **82**, 3921 (1985).

[34] A. C. Parr, S. H. Southworth, J. L. Dehmer, and D. M. P. Holland, Nucl. Instrum. Methods Phys. Res. **222**, 221 (1984).

[35] D. M. P. Holland, J. B. West, A. A. MacDowell, I. H. Munro, and A. G. Beckett, Nucl. Instrum. Methods Phys. Res. B **44**, 233 (1989).

[36] J. B. West and H. A. Padmore, in *Handbook on Synchrotron Radiation*, Vol. II, edited by G. V. Marr (North-Holland, Amsterdam, 1987), p. 21.

[37] V. G. Horton, E. T. Arakawa, R. N. Hamm, and M. W. Williams, Appl. Opt. **8**, 667 (1969).

[38] D. M. P. Holland, A. C. Parr, D. L. Ederer, J. L. Dehmer, and J. B. West, Nucl. Instrum. Methods **195**, 331 (1982).

[39] C. N. Yang, Phys. Rev. **74**, 764 (1948).

[40] J. W. Cooper and R. N. Zare, *Lectures in Theoretical Physics*, Vol. XI-C, edited by S. Geltman, K. T. Mahanthappa, and W. E. Brittin (Bordon and Brach, New York, 1968), p. 317.

[41] J. A. R. Samson and A. F. Starace, J. Phys. B **8**, 1806 (1975).

[42] J. L. Gardner and J. A. R. Samson, J. Electron Spectrosc. **13**, 7 (1978).

[43] J. E. Hardis, T. A. Ferrett, S. H. Southworth, A. C. Parr, P. Roy, J. L. Dehmer, P. M. Dehmer, and W. A. Chupka, J. Chem. Phys. **89**, 812 (1988).

[44] B. Leyh, J. Delwiche, M.-J. Hubin-Franskin, and I. Nenner, Chem. Phys. **115**, 243 (1987).

[45] B. Leyh, G. Raseev, M.-J. Hubin-Franskin, J. Delwiche, H. Lefebvre-Brion, I. Nenner, P. Roy, and J. E. Collin, in *Photophysics and Photochemistry above 6 eV* (Elsevier, Amsterdam, 1985), p. 33.

[46] G. V. Marr, J. M. Morton, R. M. Holmes, and D. G. McCoy, J. Phys. B **12**, 43 (1979), and references therein.

[47] J. W. Davenport, Phys. Rev. Lett. **36**, 945 (1976).

[48] S. Kakar, H. C. Choi, and E. D. Poliakoff, Chem. Phys. Lett. **190**, 489 (1992).

[49] J. A. Stephens and D. Dill, Phys. Rev. A **31**, 1968 (1985).

[50] R. R. Lucchese and R. W. Zurales, Phys. Rev. A **44**, 291 (1991).